^{13}C NMR study of the magnetic properties of the quasi-one-dimensional conductor $(TMTTF)_2SbF_6$

F. Iwase,[1,*] K. Sugiura,[2] K. Furukawa,[1,2] and T. Nakamura[1,2]
[1]*Institute for Molecular Science, Myodaiji, Okazaki, 444-8585, Japan*
[2]*The Graduate University for Advanced Studies, Myodaiji, Okazaki, 444-8585, Japan*
(Received 29 June 2011; published 26 September 2011)

Magnetic properties in the quasi-one-dimensional organic salt, $(TMTTF)_2SbF_6$, where TMTTF is tetramethyltetrathiafulvalene, are investigated by ^{13}C NMR under pressures. Antiferromagnetic phase transition at ambient pressure (AFI) is confirmed. Charge ordering is suppressed by pressure and is not observed under 8 kbar. For $5 < P < 20$ kbar, a sharp spectrum and the rapid decrease of the spin-lattice relaxation rate $1/T_1$ were observed below about 4 K, which is attributed to a spin-gap transition. Above 20 kbar, an extremely broadened spectrum and a critical increase of $1/T_1$ were observed. This indicates that the system enters into another antiferromagnetic phase (AFII) under pressure. The slope of the antiferromagnetic phase transition temperature T_{AFII}, dT_{AFII}/dP, is positive, while T_{AFI} decreases with pressure. The magnetic moment is weakly incommensurate with the lattice at 30 kbar.

DOI: 10.1103/PhysRevB.84.115140 PACS number(s): 71.20.Rv, 71.30.+h, 71.45.Lr, 76.60.−k

I. INTRODUCTION

Quasi-one-dimensional (1D) organic conductors, $(TMTCF)_2X$ (C = S, Se), are of interest for various electronic phases, such as charge ordering (CO), spin Peierls (sP), antiferromagnetic (AF), incommensurate spin-density wave (IC-SDW), and superconductivity (SC), by substituting anion X and pressure.[1–3] Many-body interactions, including correlated electrons and electron-phonons, are the origin of the variety of the phases. A hallmark of the extensive experimental research is a generalized phase diagram.[3,4] At high temperatures, tetramethyltetrathiafulvalene (TMTTF) salts are in a metallic state with 1/4-filled band, constructed from a TMTTF molecular π orbital. A metal-insulator crossover takes place by lowering the temperature below about 200 K (Ref. 5) due to Umklapp scattering.[6] In the insulating state, an anomaly in thermopower and resistivity was discussed in terms of a *structureless transition*,[7] which is now understood as the CO transition (or 4-k_F charge density wave, where k_F is the Fermi wave vector). Observations of an anomaly in dielectric permittivity[8–10] and line splitting of the NMR spectrum[11] are strong evidence of the CO transition. Analysis of the anisotropy of the electron spin resonance (ESR) line width ΔH_{pp} indicates that the CO pattern along the stacking axes is –O–o–O–o (where O denotes a charge-rich site and o denotes a charge-poor site).[12] The CO transition temperature T_{CO} strongly depends on the size of the anions, and also depends on the degree of the dimerization of TMTTF molecules or the strength of the electronic correlations.[13] The values of T_{CO} for PF_6, AsF_6, and SbF_6 are 65, 100, and 157 K, respectively. The driving force of the CO is regarded as the energy balance of the on-site Coulomb repulsion U, next-neighbor Coulomb repulsion V, and transfer integral t.[14–16] On the other hand, it was pointed out that the effect of the Coulomb interaction is not enough to produce the CO state in the real material.[17] Many theoretical studies have discussed that the CO state can be stabilized by the shift of the anions.[18–23] The displacement of anions is experimentally indicated by the structural investigation.[24] However, the effect of the anions is secondary for the CO transition when we consider the behavior of an anion ordering (AO). ReO_4 salt shows the AO and CO separately at $T_{AO} = 158$ K and $T_{CO} = 225$ K, respectively.[23,25] The deutration to TMTTF molecules increases T_{CO}, whereas T_{AO} remains unchanged.[26,27] This implies that the correlation between the CO and the anion is weak. Applying pressure decreases the T_{CO},[22,28,29] due to the increase of t.

At the lower pressure portion of the generalized phase diagram presented in Ref. 3, there is the sP (or spin-gap (SG)) phase.[30–35] $(TMTTF)_2PF_6$ shows the CO transition above the temperature of the sP transition. In the sP phase, the CO state has been detected by the ^{13}C NMR under the high magnetic field.[29,36,37] Many theoretical studies have proposed the possibility of the coexistence of the CO and sP.[17,19,20,38] However, the amplitude of the charge separation considerably decreases in the sP phase.[30,38,39]

The title complex $(TMTTF)_2SbF_6$ is expected to be located in the lower portion of the phase diagram, based on its large lattice parameter.[4,28] Therefore, this complex is suitable for the study of the whole range of the phase diagram. The crystal structure is shown in Fig. 1. The unit cell has two TMTTF molecules, including an inversion center ($P\bar{1}$). The SC phase was observed in a wide pressure range under extreme high pressures of $5.4 < P \leqslant 9$ GPa.[4] The value of T_{CO} at ambient pressure is ∼157 K, evidenced by dielectric susceptibility,[18,22,40] ESR,[12] and NMR.[28,41] The ratio of the charge separation estimated by ^{13}C NMR is about 3:1.[41] The ground state at ambient pressure of $(TMTTF)_2SbF_6$ is an AF ($T_{AF} \sim 7.5$ K).[42,43] The striking observation of the AF phase rather than the sP phase at ambient pressure has cast doubt on the assumption that the dimensionality of the system increases with increasing pressure.[4,35] The sP phase transition can be explained by the one-dimensional Heisenberg dimer model.[44] Therefore, the forming of the sP phase by applying hydrostatic pressure as breaking the three-dimensional AF order is not easily understood, while the existence of the sP phase has been explained by two-dimensional ^{13}C NMR.[28,41] The comprehensive studies of the magnetic properties of the electronic ground states and the detailed electronic interactions are required. A second AF phase in $(TMTTF)_2SbF_6$ (AFII

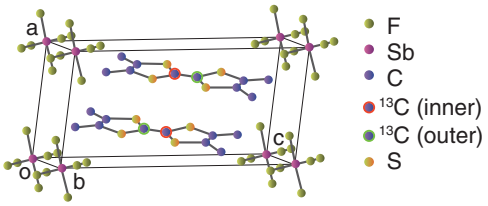

FIG. 1. (Color online) Crystal structure of $(TMTTF)_2SbF_6$. Two carbons in a TMTTF molecule are ^{13}C enriched.

phase), which is expected at higher than the sP phase, has not been reported.

In this paper, the variation in the magnetic ground states of $(TMTTF)_2SbF_6$ is investigated by applying physical pressure using standard 1D ^{13}C NMR. The CO is clearly observed by the NMR line splitting. The value of T_{CO} decreases with increasing pressure. At about 8 kbar, the CO is not detected. For $5 < P < 20$ kbar, a spin-gap state is observed in the reduction of the spin-lattice relaxation rate $1/T_1$ below about 4 K. Above 20 kbar, the ground state enters into another AF phase (AFII). The broadened spectrum suggests that the magnetic moment in the AFII phase is weakly incommensurate with the lattice.

II. EXPERIMENT

Single-crystal samples of TMTTF molecules with ^{13}C at double-bonded carbons (see Fig. 1) were prepared for NMR measurements using a standard electrocrystallization method.[12,25,45–47] A hybrid NiCrAl-BeCu clamp-type pressure cell was used to apply pressure. Daphne 7373 and 7474 were used as the pressure media for hydrostatic pressure in the pressure ranges of $P < 20$ and $P > 20$ kbar, respectively. The pressures given in this report were measured at room temperature. The reduction in the internal pressure at low temperatures is less than 2 kbar for Daphne 7373 and 2.7 kbar for Daphne 7474.[48] We developed a NMR probe which can rotate the sample around the molecular stacking a axis with the pressure cell. An external field of 8 T (~86 MHz) was applied at the magic angle such that additional line splitting originating from $^{13}C = {}^{13}C$ dipolar coupling (Pake doublet) vanished. The NMR spectrum was obtained by taking the fast Fourier transform of the signal obtained after applying a $(\pi/2)$-(π) spin-echo pulse sequence. The typical $(\pi/2)$ pulse width is 2.8 μs. The spin-lattice relaxation rate $1/T_1$ was measured by the saturation recovery method.

III. RESULTS AND DISCUSSION

A. Charge ordering and antiferromagnetic phase transition at ambient pressure

Figure 2 shows the temperature dependence of the ^{13}C NMR spectrum at ambient pressure. The spectrum consists of two narrow lines at high temperatures. NMR shift K_{obs} is expressed as $K_{obs} = K_s + K_{orb}$, where K_s is the Knight shift, and K_{orb} is the chemical shift. K_s is related to the spin susceptibility χ_s by the hyperfine coupling constant A as $K_s = A\chi_s$. Two lines observed at high temperatures are originated from two inequivalent ^{13}C sites with different A and K_{orb} in a TMTTF molecule (crystallographically inequivalent

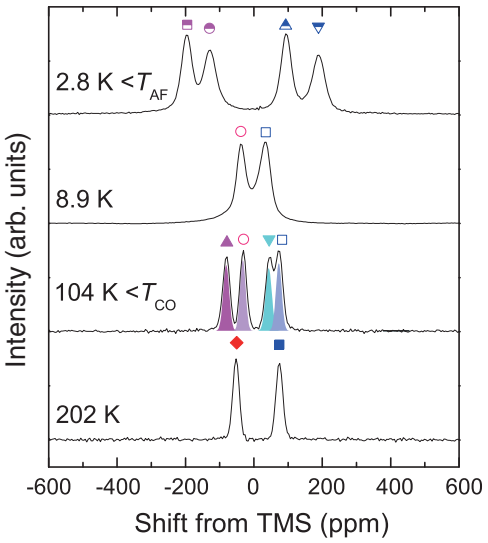

FIG. 2. (Color online) Temperature dependence of the ^{13}C NMR spectrum of $(TMTTF)_2SbF_6$ at ambient pressure.

inner and outer ^{13}C sites). On cooling, each line splits into two lines due to the CO below $T_{CO} \approx 158$ K. The CO makes two TMTTF molecules on a unit cell inequivalent.

The amplitude of the charge separation below T_{CO} can be estimated by the measurement of the spin-lattice relaxation rate $1/T_1$. In the paramagnetic state, $1/T_1$ is written as $1/T_1 = \frac{2\gamma_n^2}{\mu_B^2}\sum_q (A_q A_{-q})_\perp \frac{\mathrm{Im}\chi_\perp(\mathbf{q},\omega_n)}{\omega_n}$, where γ_n is gyromagnetic ratio of the ^{13}C nuclear, μ_B is Bohr magneton, A_q is the q dependent hyperfine coupling, ω_n is the Larmor frequency (~86 MHz), and $\mathrm{Im}\chi_\perp$ is the imaginary part of the dynamical susceptibility perpendicular to the external magnetic field.[49] We assume here that the weak site dependence of $\mathrm{Im}\chi_\perp(\mathbf{q},\omega_n)$, isotropic A_q (A), and $A \propto \rho$, where ρ is the charge density, results in $1/T_1$ that is roughly proportional to ρ^2. $A \propto \rho$ is reliable because we consider here just one band (π orbital). The recovery curve of the nuclear magnetic relaxation is obtained for each site by integrating the intensity of the spectrum. As the recovery curve cannot be fitted by a single exponential function near the antiferromagnetic critical region, we used a stretched exponential function $[M(\infty) - M(t)]/M(\infty) = \exp[-(t/T_1)^\lambda]$, where λ parametrizes the distribution of $1/T_1$ in order to discuss the temperature dependence of $1/T_1$ in the whole temperature range. At 202 K, the values of $1/T_1$ for the higher and lower signals are estimated to be 115 s^{-1} and 45.7 s^{-1}, respectively. This indicates that the higher signal is from the inner ^{13}C site in the TMTTF molecule, while the lower signal originates from the outer site (see Fig. 1), since ρ tends to be large near the center of the stacking chain. The temperature dependence of $1/T_1$ is shown in Fig. 3(a). The value of $1/T_1$ decreases with decreasing temperature above T_{CO}. The feature of the temperature dependence around T_{CO} agrees with that of the earlier report.[41] We estimated the amplitude of the charge separation by using the ratio of $1/T_1$ for split lines below T_{CO}.[50] In the inset of Fig. 3(a), the temperature dependence of $\sqrt{(1/T_1^R)/(1/T_1^P)}$, where T_1^R (T_1^P) is the relaxation time of the rich (poor) site, is shown. The ratio of the estimated charge separation is about 3.5:1 at 50 K, which is close to the previously obtained ratio of 3:1.[41]

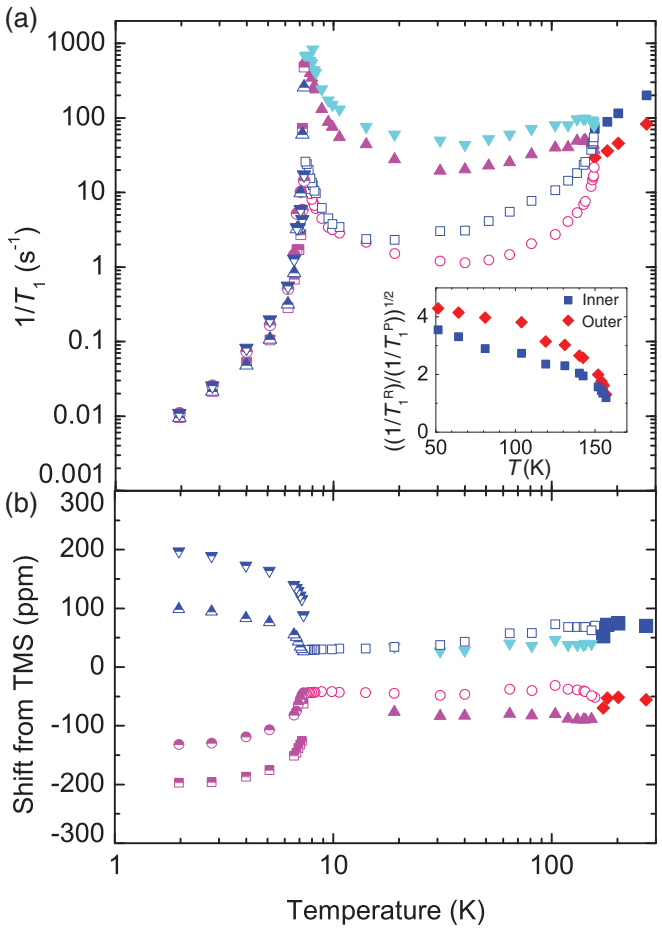

FIG. 3. (Color online) (a) Temperature dependence of $1/T_1$. (b) Temperature dependence of the peak positions in the NMR spectrum. The NMR shift is measured from the tetramethylsilane (TMS) signal. The symbols are the same as those in the spectrum in Fig. 2.

Figure 3(b) shows the temperature dependence of the peak positions of the ^{13}C NMR spectra; the symbols correspond to those in the spectra in Fig. 2. Near T_{CO}, many physical properties in the system are governed by the critical behavior of the CO transition. The amplitude of the charge separation is also reflected in the degree of the NMR line splitting $\Delta K(T)$ below T_{CO}. At T_{CO}, both K_s and K_{orb} for the inner and outer ^{13}C nuclei will change critically due to the CO, resulting in the line splitting. When we assume K_s and K_{orb} follow a power law $(T_{CO} - T)^{\beta}$, where β is a symmetry-breaking critical exponent, $\Delta K(T)$ is written as $\Delta K(T) \propto (T_{CO} - T)^{\beta}$. Figure 4 shows the temperature dependence of $\Delta K(T)$ below T_{CO}. The order parameter can be characterized by a critical exponent β. $\beta \sim 0.28$ is derived by fitting in the temperature range from 149 to 157.5 K for $T_{CO} = 157.707$ K, which is the fitting parameter. This value is smaller than $\beta = 0.5$ for the mean-field value and $\beta = 0.325 \pm 0.001$ for the 3D Ising model.[51] The early works suggested the mean-field value.[11,29] Our precise estimation indicates that $\Delta K(T)$ rises rapidly just below T_{CO}, whereas the CO transition seems to occur almost continuously. Although we do not exclude the possibility that the CO transition is of the first order, the rapid rise suggests that there is another mechanism for the transition, which

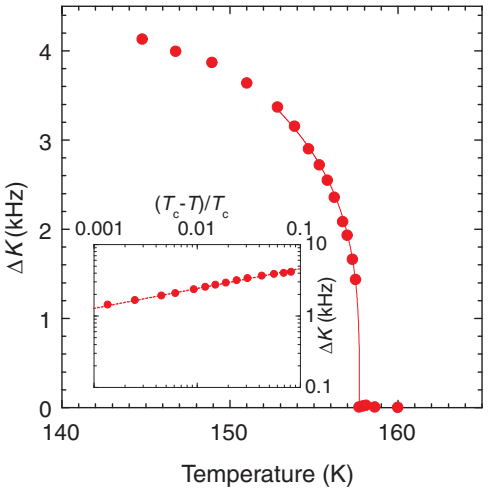

FIG. 4. (Color online) Temperature dependence of the line splitting $\Delta K(T)$ of ^{13}C NMR spectrum below T_{CO}. In the inset, $\Delta K(T)$ is plotted as a function of the reduced temperature.

determines the nature of the phase transition, other than the Coulomb interaction along the one-dimensional chain (e.g., the shift of anions).

Upon cooling, additional line splitting occurs below $T_{AF} \approx 7.5$ K, as shown in Fig. 2(a). The symmetric line splitting is attributable to the staggered moment in the AF phase. The well-separated peaks indicate that the spin configuration is commensurate with the lattice. Above T_{AF}, four lines originated from the CO merge into two lines, with decreasing temperature. $1/T_1$ for the charge-rich site $1/T_1^R$, and the charge-poor site $1/T_1^P$, are separated by fitting the recovery curve of the nuclear relaxation with the double exponential function $[M(\infty) - M(t)]/M(\infty) = A\{\exp[-(t/T_1^R)] + \exp[-(t/T_1^P)]\}$ for two lines. The value of $1/T_1$, represented in Fig. 3, increases below about 30 K and shows a pronounced peak at T_{AF}. This is caused by the critical slowing down of the antiferromagnetic spin fluctuations, considering $1/T_1$ can detect the correlation of spin fluctuations at Larmor frequency.

B. Reduction of T_{CO} under pressure

Next, we discuss the CO transition under pressure. Figure 5(a) shows the temperature dependence of the spectrum at 5 kbar. At this pressure, the line splitting due to the CO occurs below $T_{CO} \sim 110$ K. The CO phase transition eventually disappears at 8 kbar, as shown in Fig. 5(b). This behavior is simply explained by the decrease of V/t by pressure. The overlapping of the spectra below T_{CO}, which suggests the small charge separation, prevents the estimation of the CO order parameter. In Fig. 6, the temperature dependence of $1/T_1$ measured at 5 kbar is shown. In the metallic state at high temperatures, the itinerant electrons mainly contribute to the relaxation. In this condition, $1/T_1$ is written as $1/T_1 = \pi A^2 N(E_F)^2 T$, where A is the average of the q-dependent hyperfine coupling constant, and $N(E_F)$ is the density of the state at Fermi energy E_F. The fact that the value of $1/T_1$ for inner and outer ^{13}C sites is smaller than that at ambient pressure is attributable to the decrease of $N(E_F)$ due to the increase of

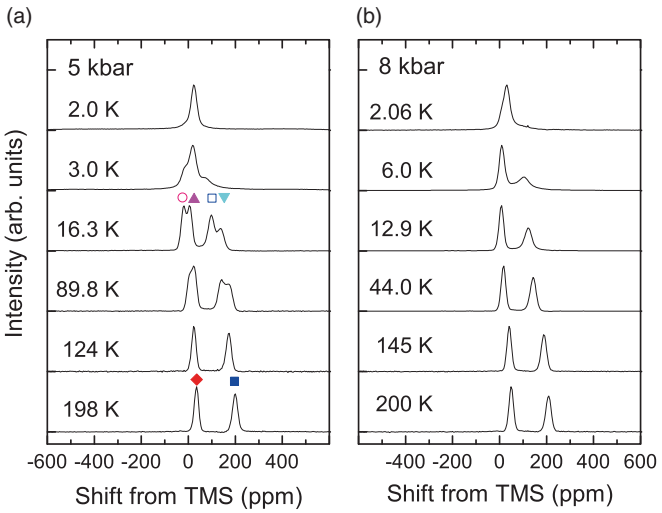

FIG. 5. (Color online) Temperature dependence of the ^{13}C NMR spectrum of $(TMTTF)_2SbF_6$ at (a) 5 kbar and (b) 8 kbar.

the band width $W(\propto t)$. Below T_{CO}, we estimate the charge separation by the ratio of $1/T_1$ in the same manner with the ambient pressure (see the inset of Fig. 6). $\sqrt{(1/T_1^R)/(1/T_1^P)}$ increases below T_{CO}, and saturates near 10 K. The charge separation is roughly in the ratio of 2:1, which is lower than the value at ambient pressure. This also indicates that the CO is destabilized by the pressure.

C. Spin-gap transition under pressure

The spectrum obtained at 5 kbar exhibits completely different features from that at ambient pressure. Below about 3 K, the spectrum forms a sharp peak. The diminishing of the site dependence of the NMR shift is caused by the reduction of spin susceptibility, $\chi_s \to 0$, considering $K_s = A\chi_s$. AsF_6, PF_6, and I salts have similar spectral shape below T_{sP} (or spin-singlet transition temperature T_{SS}).[29,30,35–37,39] A previous ^{13}C 2D NMR study obtained split spectra under 6 kbar on the dipolar coupling axis, which is attributed to the sP

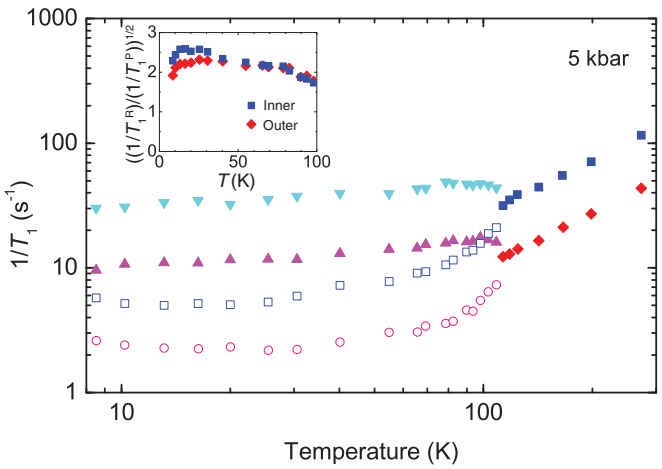

FIG. 6. (Color online) Temperature dependence of $1/T_1$ under 5 kbar.

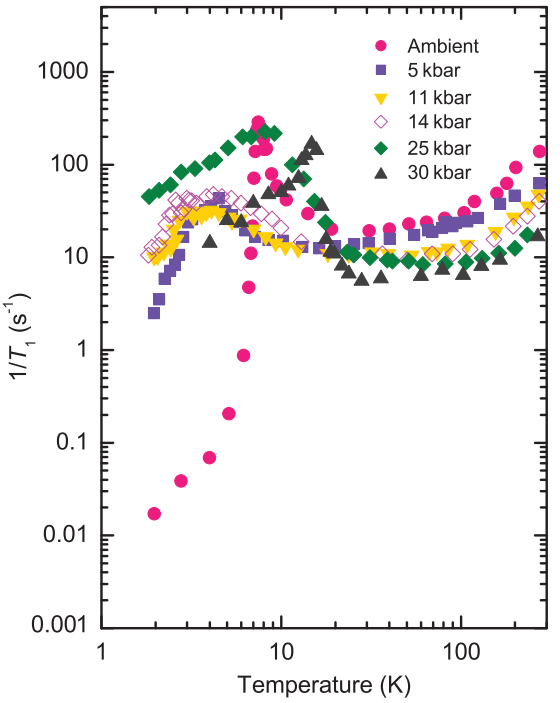

FIG. 7. (Color online) Temperature dependence of the spin-lattice relaxation rate $1/T_1$ at six different pressures.

state.[28] The single line spectrum is also observed at 8 and 11 kbar, as shown in Figs. 5(b) and 8(a). The temperature dependence of $1/T_1$ under various pressures is shown in Fig. 7. Here, $1/T_1$ was defined as the initial slope of the relaxation curve of nuclear magnetization after saturation. This estimation characterizes the volume average of $1/T_1$. The striking feature is the suppression of the critical increase in $1/T_1$ observed near T_{AF}. The value of $1/T_1$ shows a drop below about 3–4 K without significant peak structure, which is attributable to a spin-gap transition. Although it is difficult to conclude whether or not the spin gap is opened, because the temperature range measured below the anomaly is too narrow and prevents the characterization of the gap structure, here we attribute this behavior to a spin-gap transition, considering the similarity with that in the other TMTTF complexes. The gap size is $\Delta/k_B \sim 8$ K, estimated by using the data of $1/T_1$ under 11 kbar, just below the spin-gap transition temperature, and assuming that $1/T_1$ follows an activation type $1/T_1 \propto \exp(-\Delta/k_BT)$.

However, the NMR shift has a different character. Figure 8(c) shows the temperature dependence of the resonance frequency at the peak position and the center of gravity of the spectra (first moment) at 11 kbar. The first moment monotonically decreases with decreasing temperature. In TMTTF salts, as the Knight shift is negative in the paramagnetic state, a positive shift is expected below the sP transition.[25,30,39,52] The reason for the shift to lower frequencies, which is the opposite direction for the nonmagnetic spin-singlet state, is not clear at this moment. Our observation indicates that there is no reduction in χ_s. Even though the local spin susceptibility at the outer ^{13}C site [indicated by the diamond symbols in Fig. 8(c)] appears to decrease with decreasing temperature below 10 K, the first moment shows

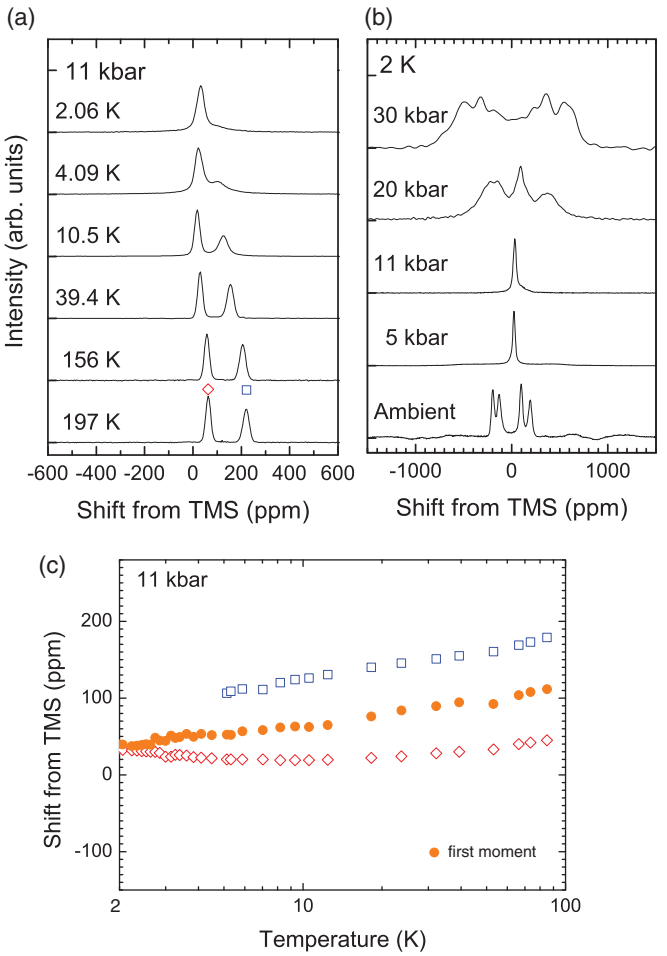

FIG. 8. (Color online) Temperature dependence of the ^{13}C NMR spectrum of $(TMTTF)_2SbF_6$ under (a) 8 kbar and (b) 11 kbar. (c) Temperature dependences of the peak position and center of gravity (first moment) of the ^{13}C NMR spectrum at 11 kbar. The symbols are the same as those in the spectrum in (a).

no anomaly at the temperature. It is possible that $K_{\rm orb}$ (or Knight shift origin) is modulated by the external pressure. As a result, $K_{\rm orb}$ becomes lower and the sign of A changes from negative to positive. The shift origin can be estimated by an analysis of the $K_{\rm obs}$ versus spin susceptibility χ plot under pressures. The investigation of the spin susceptibility χ_s under pressure is under way.

The coexistence of the CO and sP orderings is claimed to be evidenced by the broadened spectrum of ^{13}C NMR in $(TMTTF)_2PF_6$ at 21.0 T.[29] Our experiment could not detect the coexistence, as the magnetic field in our experiment is 9 T, which is lower than the critical field B_c for the triplet excitations.

D. Antiferromagnetic ordering under pressure

Above 20 kbar, the spectrum shows a different feature at low temperatures. Figure 8(b) shows the pressure dependence of the ^{13}C NMR spectrum at 2.0 ± 0.1 K. The spectrum exhibits significant broadening above 20 kbar. This behavior indicates that the system enters into the expected AFII phase. $1/T_1$, estimated at the center of the spectrum, shows the critical increase near the transition temperature $T_{\rm AFII}$, as shown in Fig. 7, supporting the AFII transition. The spectral shape is different from that for the AFI phase, in which four peaks are well separated. The spectral profile exhibits some characteristics of weak incommensurability with the lattice, namely, a wide distribution ($\pm$500 ppm) at 30 kbar, a substantial spectral density at the center of the spectrum, and a narrow tail compared to that at 20 kbar. The value of $1/T_1$ decreases below $T_{\rm AFII}$ gradually compared to the reduction at ambient pressure. If the ground state is incommensurate spin-density wave (IC-SDW), then the *gradual* decrease of $1/T_1$ below $T_{\rm AFII}$ is attributable to the phason mode, which dominates spin-lattice relaxation in the IC-SDW phase.[53] $1/T_1$ of the side wings of the spectrum for the IC-SDW phase corresponds to the relaxation due to the amplitude modes. As we estimated $1/T_1$ only at the central part of the spectrum, we cannot discuss the difference of the $1/T_1$ between the central part and the wing part of the spectrum at present. This analysis is planned for the future. The one-dimensional IC-SDW phase is expected to have a sinusoidal NMR spectrum, whereas the observed line shape at 30 kbar is not sinusoidal, suggesting that commensurate domains remain. In fact, the ground state is expected to be the commensurate AF phase driven by the spin interaction because the charge gap is opened at 30 kbar ($T_\rho > 0$) (Ref. 4) for which the spin-localized picture is appropriate. Our observation suggests that the system is near the metal-insulator boundary above $T_{\rm AFII}$. The AF ordering patterns of AFI and AFII in $(TMTTF)_2SbF_6$ is an important topic for future studies.

E. Phase diagram

In $(TMTTF)_2SbF_6$, the behaviors of the AF and CO transitions under low pressures below 5 kbar have been established.[28] Above the $T_{\rm CO}$, a metal-insulator crossover has been reported.[4,54–57] Figure 9 shows a phase diagram of $(TMTTF)_2SbF_6$ that summarizes the results of the present study. The value of $T_{\rm CO}$ decreases with increasing pressure, which is consistent with the previous study.[28] At 8 kbar, we

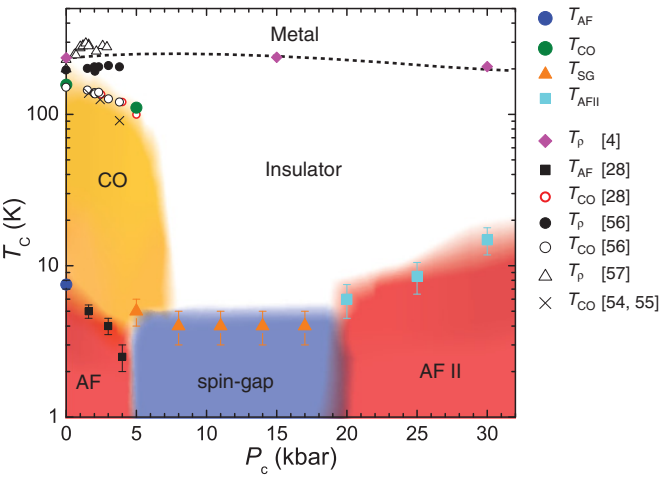

FIG. 9. (Color online) Pressure-temperature phase diagram of $(TMTTF)_2SbF_6$ constructed based on NMR measurements at hydrostatic pressures. Data from Refs. 4,28,54–57 are also shown.

could not find the CO transition. Under $5 < P < 20$ kbar, the system shows the SG phase transition below about 4 K. The existence of the singlet phase has been suggested in Ref. 28, although the transition temperature has not been established. If this state is a nonmagnetic sP phase, the sequence of the ground states contradicts the pressure effect on the dimensionality of the system.[4,35] In our experiment, the expected reduction of the Knight shift has not been observed below T_{SG}. As pointed out in Ref. 35, the interchain coupling probably plays an important role for the realization of the unconventional spin-gap phase. We observed the evidence of the AFII phase transition, which has been expected in Ref. 28. The phase transition temperature of the AFII phase, T_{AFII}, is defined as the peak of $1/T_1$. The value of T_{AFII} increases with increasing pressure as $dT_{AFII}/dP \sim +8.5$ K/kbar. In the charge-gap state, the increase in T_{AF} can be attributed to an increase in interchain spin coupling with pressure,[58] as discussed in $(TMTTF)_2Br$ at moderate pressures of below 5 kbar.[58,59] The increase of the dynamic susceptibility $\chi(2k_F)$ near T_{AFII} becomes significant with increasing pressure, as seen in the $1/T_1$ data [$1/T_1 \propto \mathrm{Im}\chi(2k_F)$ near T_{AFII}]. On further increasing the pressure, a reduction in T_{AFII} and a clear IC spin-density wave (SDW) phase are expected to be observed due to imperfect nesting in the SDW state.[60] In this situation, $\chi(2k_F)$ will reduce with pressure on approaching the SC phase as observed in $(TMTSF)_2PF_6$.[61] The observation of the widely distributed superconducting phase ($5.4 < P < 9$ GPa) (Ref. 4) is consistent with this scenario.

IV. CONCLUSION

In conclusion, we conducted ^{13}C NMR under pressures to study the magnetic properties of quasi-one-dimensional complex $(TMTTF)_2SbF_6$. NMR measurements revealed the magnetic property and the criticality of the CO transition. For $5 < P < 20$ kbar, the observations of the rapid decrease of $1/T_1$ and the spectral change suggest that the ground state is the SG state. We found an AFII phase above 20 kbar. The value of T_{AFII} increases with increasing pressure in the measured pressure range. The broadened spectrum above 30 kbar suggests that the magnetic moment tends to be incommensurate with the lattice at higher pressures.

ACKNOWLEDGMENTS

The authors wish to thank Y. Shimizu, T. Ito, H. Seo, M. Itoi, K. Yonemitsu, P. Monceau, T. Takahashi, and H. Fukuyama for valuable discussions. This study was supported by Grants-in-Aid for Scientific Research (B) (Grant No. 20340095) from JSPS, and by the Scientific Research on Innovative Areas (Grant No. 21110523) from the Ministry of Education, Culture, Sports, Science and Technology, Japan. This work was also partially supported by Grants-in-Aid for Scientific Research for Young Scientists (B) (Grant No. 23740273), and by Grants-in-Aid for Scientific Research "New Frontier of Materials Science Opened by Molecular Degrees of Freedom" (Grant No. 21110523) and for Young Scientists (A) (Grant No. 21685021) from JSPS.

*Present address: Department of Physics, Okayama University, Okayama 700-8530, Japan.

[1] D. Jérome, Chem. Rev. **104**, 5565 (2004).
[2] T. Ishiguro, K. Yamaji, and G. Saito, *Organic Superconductors*, 2nd ed. (Springer-Verlag, Berlin/Heidelberg, 1998).
[3] D. Jérome, Science **252**, 1509 (1991).
[4] M. Itoi, C. Araki, M. Hedo, Y. Uwatoko, and T. Nakamura, J. Phys. Soc. Jpn. **77**, 023701 (2008).
[5] R. Laversanne, C. Coulon, B. Gallois, J. P. Pouget, and R. Moret, J. Phys. Lett. **45**, L393 (1984).
[6] V. J. Emery, R. Bruinsma, and S. Barisić, Phys. Rev. Lett. **48**, 1039 (1982).
[7] C. Coulon, S. S. P. Parkin, and R. Laversanne, Phys. Rev. B **31**, 3583 (1985).
[8] F. Nad, P. Monceau, and J.-M. Fabre, Eur. Phys. J. B **3**, 301 (1998).
[9] F. Nad, P. Monceau, and J.-M. Fabre, J. Phys. IV **9**, Pr10–361 (1999).
[10] F. Nad, P. Monceau, C. Carcel, and J.-M. Fabre, Phys. Rev. B **62**, 1753 (2000).
[11] D. S. Chow, F. Zamborszky, B. Alavi, D. J. Tantillo, A. Baur, C. A. Merlic, and S. E. Brown, Phys. Rev. Lett. **85**, 1698 (2000).
[12] T. Nakamura, J. Phys. Soc. Jpn. **72**, 213 (2003).
[13] Y. Nogami, T. Ito, K. Yamamoto, N. Irie, S. Horita, T. Kambe, N. Nagao, K. Oshima, N. Ikeda, and T. Nakamura, J. Phys. IV **131**, 39 (2005).
[14] J. E. Hirsch and D. J. Scalapino, Phys. Rev. Lett. **50**, 1168 (1983).
[15] J. E. Hirsch and D. J. Scalapino, Phys. Rev. B **27**, 7169 (1983).
[16] H. Seo and H. Fukuyama, J. Phys. Soc. Jpn. **66**, 1249 (1997).
[17] M. Kuwabara, H. Seo, and M. Ogata, J. Phys. Soc. Jpn. **72**, 225 (2003).
[18] P. Monceau, F. Y. Nad, and S. Brazovskii, Phys. Rev. Lett. **86**, 4080 (2001).
[19] J. Riera and D. Poilblanc, Phys. Rev. B **62**, 16243 (2000).
[20] J. Riera and D. Poilblanc, Phys. Rev. B **63**, 241102 (2001).
[21] S. Brazovskii, P. Monceau, and F. Nad, Synth. Met. **137**, 1331 (2003).
[22] F. Nad and P. Monceau, J. Phys. Soc. Jpn. **75**, 051005 (2006).
[23] F. Nad and P. Monceau, J. Phys. IV **12**, Pr9–133 (2002).
[24] M. de Souza, P. Foury-Leylekian, A. Moradpour, J.-P. Pouget, and M. Lang, Phys. Rev. Lett. **101**, 216403 (2008).
[25] T. Nakamura, K. Furukawa, and T. Hara, J. Phys. Soc. Jpn. **75**, 013707 (2006).
[26] K. Furukawa, T. Hara, and T. Nakamura, J. Phys. Soc. Jpn. **74**, 3288 (2005).
[27] F. Nad, P. Monceau, T. Nakamura, and K. Furukawa, J. Phys. Condens. Matter **17**, L399 (2005).
[28] W. Yu, F. Zhang, F. Zamborszky, B. Alavi, A. Baur, C. A. Merlic, and S. E. Brown, Phys. Rev. B **70**, 121101(R) (2004).
[29] F. Zamborszky, W. Yu, W. Raas, S. E. Brown, B. Alavi, C. A. Merlic, and A. Baur, Phys. Rev. B **66**, 081103(R) (2002).
[30] S. Fujiyama and T. Nakamura, J. Phys. Soc. Jpn. **75**, 014705 (2006).
[31] M. Dumm, B. Salameh, M. Abaker, L. K. Montgomery, and M. Dressel, J. Phys. IV **114**, 57 (2004).

[32]P. Foury-Leylekian, D. Le Bolloc'h, B. Hennion, S. Ravy, A. Moradpour, and J.-P. Pouget, Phys. Rev. B **70**, 180405(R) (2004).
[33]P. Foury-Leylekian, S. Petit, C. Coulon, B. Hennion, A. Moradpour, and J.-P. Pouget, Physica B **404**, 537 (2009).
[34]M. de Souza, A. Brühl, J. Müller, P. Foury-Leylekian, A. Moradpour, J.-P. Pouget, and M. Lang, Physica B **404**, 494 (2009).
[35]K. Furukawa, K. Sugiura, F. Iwase, and T. Nakamura, Phys. Rev. B **83**, 184419 (2011).
[36]S. E. Brown, W. G. Clark, B. Alavi, D. S. Chow, C. A. Merlic, and D. J. Tantillo, Synth. Met. **103**, 2056 (1999).
[37]S. E. Brown, W. G. Clark, F. Zamborszky, B. J. Klemme, G. Kriza, B. Alavi, C. Merlic, P. Kuhns, and W. Moulton, Phys. Rev. Lett. **80**, 5429 (1998).
[38]R. T. Clay, R. P. Hardikar, and S. Mazumdar, Phys. Rev. B **76**, 205118 (2007).
[39]T. Nakamura, K. Furukawa, and T. Hara, J. Phys. Soc. Jpn. **76**, 064715 (2007).
[40]H. H. S. Javadi, R. Laversanne, and A. J. Epstein, Phys. Rev. B **37**, 4280 (1988).
[41]W. Yu, F. Zamborszky, B. Alavi, A. Baur, C. A. Merlic, and S. E. Brown, J. Phys. IV (France) **114**, 35 (2004).
[42]A. Maaroufi, S. Flandrois, G. Fillion, and J. P. Morand, Mol. Cryst. Liq. Cryst. **119**, 311 (1985).
[43]C. Coulon, J. C. Scott, and R. Laversanne, Mol. Cryst. Liq. Cryst. **119**, 307 (1985).
[44]I. S. Jacobs, J. W. Bray, H. R. Hart Jr., L. V. Interrante, J. S. Kasper, G. D. Watkins, D. E. Prober, and J. C. Bonner, Phys. Rev. B **14**, 3036 (1976).
[45]J. P. Ferraris, T. O. Poehler, A. N. Bloch, and D. O. Cowan, Tetrahedron Lett. **27**, 2553 (1973).
[46]A. Mas, J.-M. Fabre, E. Torrilles, L. Giral, and G. Brun, Tetrahedron Lett. **30**, 2579 (1977).
[47]K. Bechgaard, C. S. Jacobsen, K. Mortensen, H. J. Pedersen, and N. Thorup, Solid State Commun. **33**, 1119 (1980).
[48]T. Moriya, Prog. Theor. Phys. **28**, 371 (1962).
[49]It was pointed out that the ratio of the CO estimated by $1/T_1$ is large compared to that obtained by an infrared spectroscopy in S. Hirose, A. Kawamoto, N. Matsunaga, K. Nomura, K. Yamamoto, and K. Yakushi, Phys. Rev. B **81**, 205107 (2010). A possible explanation for the difference is attributable to the ρ dependence of the dynamical spin susceptibility and/or the antiferromagnetic spin fluctuations at low temperatures.
[50]M. D. Lumsden, B. D. Gaulin, and H. Dabkowska, Phys. Rev. B **57**, 14097 (1998).
[51]F. Iwase, K. Sugiura, K. Furukawa, and T. Nakamura, Phys. Rev. B **81**, 245126 (2010).
[52]H. Yoshioka, M. Tsuchiizu, and H. Seo, J. Phys. Soc. Jpn. **76**, 103701 (2007).
[53]E. Barthel, G. Quirion, P. Wzietek, D. Jérome, J. B. Christensen, M. Jørgensen, and K. Bechgaard, Europhys. Lett. **21**, 87 (1993).
[54]M. Nagasawa, F. Nad, P. Monceau, and J. M. Fabre, Solid State Commun. **136**, 262 (2005).
[55]M. Nagasawa, F. Nad, P. Monceau, and J. M. Febre, J. Phys. IV **114**, 119 (2004).
[56]M. Nagasawa, T. Nagasawa, K. Ichimura, and K. Nomura, J. Phys. Soc. Jpn. **77**, 105002 (2008).
[57]M. Itoi, Y. Ishii, S. Takekoshi, H. Kitano, K. Matsubayashi, Y. Uwatoko, and T. Nakamura, Physica C **470**, S594 (2010).
[58]B. J. Klemme, S. E. Brown, P. Wzietek, G. Kriza, P. Batail, D. Jérome, and J. M. Fabre, Phys. Rev. Lett. **75**, 2408 (1995).
[59]M. Hisano, T. Nakamura, T. Takahashi, and G. Saito, Synth. Met. **103**, 2195 (1999).
[60]Y. Fuseya and M. Ogata, J. Phys. Soc. Jpn. **76**, 093701 (2007).
[61]F. Creuzet, C. Bourbonnais, L. G. Caron, D. Jérome, and A. Moradpour, Synth. Met. **19**, 277 (1987).